Pakistan J. Zool., vol. 58(2), pp 901-913, 2026 **DOI**: https://dx.doi.org/10.17582/journal.pjz/20240619130642

Bacterial Exopolysaccharides (EPS) and EPS-Coated Nanoparticles against Plant and Fish Pathogens

Sana Yousaf[1], Aisha Waheed Qurashi[1]*, Mawra Gohar[1], Sajida Naseem[2], Asma Abdul Latif[3], Muhammad Afzaal[4], Awais Khalid[5] and Iram Liaqat[6]*

[1]Department of Biology, Lahore Garrison University, DHA Phase 6, Lahore Pakistan.
[2]Department of Zoology, Division of Science and Technology, University of Education, Lahore
[3]Department of Zoology, Lahore College for Women University, Lahore, Pakistan.
[4]Sustainable Development Study Centre, Government College University, Lahore, Pakistan
[5]Department of Physics, College of Science and Humanities in Al-Kharj, Prince Sattam bin Abdulaziz University, Al-Kharj 11942, Saudi Arabia
[6]Microbiology Lab, Department of Zoology, Government College University, Lahore-54000, Pakistan

Article Information
Received 19 June 2024
Revised 25 December 2024
Accepted 11 January 2025
Available online 12 June 2025
(early access)
Published 23 February 2026

Authors' Contribution
SY conducted the experiments, compiled and analyzed the data, and prepared the initial manuscript. AWQ provided primary research supervision and drafted the manuscript. MG co-supervised the study, contributing to research design and methodology. IL redrafted the manuscript, critically reviewed, edited, corrected, and revised to enhance its clarity and accuracy. SN interpreted the data. AAL provided technical review and editorial support to refine the manuscript. MA contributed to data analysis and statistical validation, ensuring accuracy in results. AK provided technical assistance in manuscript drafting and revisions, improving its overall structure and coherence.

Key words
Antibiofilm, Exopolysaccharides, EPS-coated Nanoparticles, Bacteria, Plant interactions

ABSTRACT

Exopolysaccharides (EPS) are biological macromolecules, constituting the major part of biofilm and possess antibacterial and antibiofilm properties. EPS producing strains of bacteria were exploited for EPS production and antimicrobial assay against plant (HT5, HT6, and HT7) and fish (SCC4, NP4, TS1, TM4) pathogens using Kirby Bauer disc diffusion method. MIC value recorded was 0.2mg/ml against plant pathogen HT7 and further antimicrobial assay was performed using turbidity assay at optimized concentration of EPS (0.2mg/ml). Both EPS-coated and non-coated nanoparticles (NP's) were synthesized and characterized by XRD and SEM analysis. MIC value for each NP was recorded as 0.6mg/ml against HT7 and used for further analysis in turbidity assay. Biofilm formation was assessed by ring assay and maximum biofilm formation was recorded after 48 h of incubation and represented as normalized biofilm for quantitative estimation. BHIC agar (brain heart infusion agar with congo-red) was used for qualitative analysis of biofilm inhibition in presence of NP's and revealed by inhibition of brown color of colonies. Antibiofilm assay for NP's was performed at their optimized conc. using microtitre assay and significant reduction was recorded in biofilm. NP's were also exploited to determine their effect on plant growth and wheat seeds were grown in presence of NP's under stress of plant pathogens and significant improvement was observed in plant growth in presence of NP's. EPS and NP's showed promising improvement in treatment of pathogens, against biofilm producers and also helpful in improving plant growth by inhibiting plant pathogens and increasing plant biomass.

INTRODUCTION

Multiple microbial species are capable to secrete exopolysaccharides (EPS) (Castellane *et al*., 2014). These compounds are widely used in different industries e.g., food, pharmaceutical and chemical as starter culture and co-adjutant to develop fermented foods, as drug delivery agents and as bio-flocculants and bio-absorbents, respectively. Biofilms are community of different microbes grown on any surface and they possess maximum resistance towards conventional ways of treatment including antibiotics. Bacteria in biofilms are more resistant towards antimicrobial agents, approximately 1000 times as compared to free living bacteria (planktonic cells) (Mah and O'toole, 2001).

Antibiotics used for treatment, include gentamycin, rifampin, tobramycin, daptomycin and clarithromycin (Ciofu *et al*., 2017) which are least effective for the treatment of biofilm related infections. In such condition,

* Corresponding author: dr.iramliaqat@gcu.edu.pk, aishawaheedqureshi@lgu.edu.pk
0030-9923/2026/0002-0901 $ 9.00/0

the best way is the development of nanoparticles of metal oxides in order to treat drugs resistant biofilm producers (Baelo *et al*., 2015). Thus, it is a suitable agent for biofilm treatment and is widely used in hospitals and industrial settings (Allaker and Memarzadeh, 2014).

Inorganic nanoparticles (NPs) are effective antimicrobial agents and exhibit antibacterial activity due to formation and release of reactive oxygen species (ROS). They are also capable of binding with nucleic acids disturbing the cellular functions (inhibiting the process of microbial replication and protein synthesis) thus damaging the whole cell.

Inorganic NPs containing either metals or their oxides are reported to be more stable and highly effective and show maximum antibacterial activity as compared to organic NPs. Metal-based NPs are highly effective due to different functional groups present on their surface that helps to increase their interaction with target surfaces. The metal oxide NPs studied include iron oxide (Fe_2O_3), cerium oxide (CeO), zinc oxide (ZnO), magnesium oxide (MgO), aluminum oxide (Al_2O_3), copper oxide (CuO) and titanium dioxide (TiO_2) etc.

EPS can inhibit the growth of different pathogens. It is reported that exopolysaccharides (EPS) constituents produced by *Pseudomonas aeruginosa*, can effectively inhibit the growth of bacterial strains of *Bacillus subtilis* and *Escherichia coli*. The maximum zone of inhibition (25.6-26.4 mm) was observed against *Bacillus subtilis* and lowest antimicrobial activity (4.2-6.0) was observed against *Escherichia coli*. Naseem and Farrukh (2015) studied that iron NPs synthesized from leaf extract of *Gardenia jasminoides* are capable of inhibiting growth of human pathogens including *Staphylococcus aureus*, *Escherichia coli*, *Salmonella enterica*, and *Proteus mirabilis*.

Salman et al. (2015) reported that coating of iron NPs on surface of catheters can inhibit the growth of biofilm forming bacteria including *S. aureus* and *E. coli.* Growth of *C. jejuni* can be inhibited using ZnO NPs. The cells treated with ≥0.03 mg/ml of the NPs for 16 h were no longer culturable on agar plates. It was demonstrated that 0.5, 0.3, and 0.1 mg/ml of ZnO NPs resulted in complete killing (100%) of *C. jejuni* cells in 3 h or less. Hence, it was concluded that ZnO NPs are effective at killing *C. jejuni* even at low concentrations. Swain et al. (2014) studied that zinc oxide (ZnO) NPs are highly effective against fungal pathogens associated with diseases of aquaculture because of increased rate of mortalities and increased antibiotic resistance.

Study conducted by Varghese and George (2015) demonstrated that EPS stabilized iron NPs can effectively inhibit the growth of human and fish pathogens. Tested strains used for antibacterial activity were *Aeromonas hydrophila* and *Aeromonas sobria*. After incubation of 24h, results revealed that bacterial growth was inhibited with increasing conc. of NPs and MIC value was 100 µg/ml for both pathogens of fish. Hence concluded that, EPS plays important role in stabilization of iron NPs and can be used efficiently in treatment of infections as well. EPS coated ZnO NPs are highly effective antibiofilm agents against biofilm producers. MIC value of EPS-ZnO NP's was 30 µg/ml for both *B. subtilis* and *C. albicans* and 40 µg/ml for *P. aeruginosa*. EPS-ZnO NP's treated wells indicated that biofilm was weakly adhered and disintegrated and its structure was significantly reduced and damaged, confirmed by COMSAT software. Hence concluded that, EPS coated ZnO NP's are highly effective antibacterial and antibiofilm agents.

The impacts of phytopathogens on agricultural systems, disease controls and economic losses caused by the pathogens are internationally important research subjects. Recently, increasing evidence has shown that phytopathogens play a critical role in mediating competitions among their host plant species (Chen and Nan, 2015). Commercially available CuNP's were tested *in vitro* and proved to be effective against a wide range of organisms encompassing plant pathogenic and non-pathogenic fungi and bacteria (Banik and Luque, 2017).

MATERIALS AND METHODS

Bacterial strains

For EPS extraction from bacterial cultures, previously isolated and characterized EPS producing bacterial isolates named *Bacillus cereus* (EG4), *Citrobacter freundii* (IG-1), *Exigoubacterium auranticum* (EPF1), *Bacillus cereus* (HFF), *Bacillus subtilis* (HFP), *Bacillus subtilis* (HYP), *Bacillus subtilis* (HYS), *Bacillus licheniformis* (SMK), *Alkaligene faecalis* (AQ-1), *Bacillus subtilis* (NAY) were revived from glycerol stocks by inoculating loop-full into 10ml of LB-broth and incubating at 37°C for 24 h under appropriate conditions. These cultures were previously isolated by Qurashi and Co-workers in their lab and further used for EPS extraction (unpublished work).

Pathogenic isolates

Pathogenic bacterial isolates, including plant pathogens (HT5, HT6 and HT7) and fish pathogens (TS1, TM4, SCC4 and NP4) were revived from glycerol stock previously used in research were added into sterile LB-broth and incubated under proper sterile conditions.

The selection includes both plant pathogens (HT5, HT6, and HT7) and fish pathogens (TS1, TM4, SCC4, and NP4), which broadens the scope of the study. The inclusion

of both plant and fish pathogens allows for a comparative analysis of pathogen behavior, EPS production, and their roles in host-pathogen interactions across different biological systems. These strains were revived in sterile LB-broth under proper conditions, indicating that they are well-suited for growth in controlled laboratory environments. Their ability to thrive in such settings makes them appropriate candidates for experiments requiring stable, consistent bacterial cultures.

Extraction and quantification of EPS

EPS were extracted from various bacterial strains following method as described previously by Qurashi and Sabri (2016). Bacterial cultures were grown under appropriate conditions to produce EPS. The cultures were then centrifuged at 10,000 rpm for 10 min to obtain a cell-free supernatant. To precipitate EPS, the supernatant was mixed with double the volume of chilled acetone (stored at -20°C), gently mixed, and kept at 4°C for 12–24 h. The precipitated EPS, appearing as white pellets, was collected by centrifugation at 15,000 rpm for 20 min at 4°C and confirmed after comparing with control non EPS producing strains. The pellet was washed 2–3 times with distilled water to remove impurities and stored at -20°C for further use.

MIC of EPS and bacterial growth inhibition

Minimal inhibitory concentration (MIC) of EPS was determined by Kirby Bauer disc diffusion method following protocol described by Ghalem (2017). For this purpose, Mueller Hinton agar (MHA) was used and OD of test organism was adjusted 0.5 for antimicrobial activity at varying concentration of EPS including 0.2, 0.4, 0.6, 0.8, 1 mg/ml. Erythromycin (3 mg/ml) was used as positive control. After incubation for 24 h, zone of inhibition was observed and measured in terms of mm/mg of EPS. The zone diameters were compared using CLSI Chart (2018).

Turbidity assay was performed after optimizing the MIC of EPS requisite to prevent bacterial growth. This assay was performed following the method described by Lourenço and Pinto (2011) to determine antimicrobial activity of EPS against plant and fish pathogens (HT5, HT6, HT7, TS1, TM4, SCC4 and NP4). For this purpose 100 µl EPS was added into microtitre 96-well plate along with 100 µl of tested organisms (OD= 0.5) and erythromycin (3mg/ml) as positive control. After incubation, optical density (OD) was recorded spectrophotometrically at 600 nm.

Synthesis of EPS coated NPs

Iron oxide (FeO) NPs were synthesized by following protocol described by Gottimukkala *et al*. (2017) using green tea leaf extract with the modification that the precursor metal used for synthesis was $FeCl_3$. $6H_20$. Brown precipitates of NPs, settled down in bottom, were recovered by centrifugation at maximum speed at 15000 rpm for 15 min. Pellet was washed and stored at -20 °C for further use.

Zinc NPs were synthesized following protocol described by Varghese and George (2015) using aloe vera extract and zinc acetate solution. 2M NaOH solution was added in order to adjust the pH 12 of the solution. White crystalline precipitates of zinc oxide were obtained and separated out by centrifugation. Pellet was washed and stored for further use.

EPS coated iron and zinc NPs were synthesized using respective EPS of 10 strains auch as EG4, IG-1, EPF1, HFF, HFP, HYP, HYS, SMK, AQ-1 and Nay. EPS coated iron NPs were synthesized using 3M $FeCl_3$ and 3M $FeSo_4$ by following protocol described by Varghese and George (2015). Brown precipitates tend to form in bottom of flask and were recovered by centrifugation at maximum speed. Pellet was washed and then stored at -20°C for further use.

EPS coated ZnO NPs were synthesized using 2M zinc acetate and 2M NaOH solution. White precipitates of ZnO were recovered by centrifugation at maximum speed. Afterwards, pellet was washed 3 times and stored at -20°C for further use.

Characterization of NPs (iron, EPS coated iron, zinc, EPS coated zinc) was carried out by scanning electron microscopy (SEM) (TESCAN Vega- LMU– Variable pressure Scanning Electron Microscope JSM-6490) and X-ray diffraction (XRD) analysis. Samples were sent to avail commercial services and obtained spectrum results were collected.

Antimicrobial activity of non-coated and EPS-coated NPs

Antimicrobial activity of FeO and ZnO NPs and respective EPS coated NPs and only EPS (as control) was determined using Kirby Bauer disc diffusion method (Bauer *et al*., 1966). For this purpose, Mueller Hinton agar (MHA) was used and NPs were diluted accordingly as mentioned concentrations (0.2, 0.4, 0.6, 0.8, 1 mg/ml). After incubation, zones of inhibition were observed and measured in terms of mm/mg of NPs and compared using CLSI standards.

Turbidity assay was performed after optimizing the MIC of NP's requisite to prevent bacterial growth. This assay was performed following the method described by Lourenço and Pinto (2011) to determine the antimicrobial activity of NP's against plant and fish pathogens. For this purpose, 100 µl of NP's were added into each respective well along with 100 µl of tested organisms (OD_{600}= 0.5)

and erythromycin (3 mg/ml) and bacterial EPS (HFP) as positive control. After incubation, optical density (OD) of plate was recorded spectrophotometrically at 600 nm.

Qualitative assay to check efficacy of NPs on biofilm inhibition

Biofilm formation of bacterial pathogenic isolates (HT5, HT6, HT7, TS1, TM4, SCC4 and NP4) was determined by following protocol described by Fujishige *et al*. (2006) following same modifications as described of Aqsa *et al*. (2023). Biofilm formation was represented as normalized biofilm for quantitative estimation and assay was performed to optimize maximum time for biofilm synthesis.

Antibiofilm efficacy of NPs (iron and zinc) on biofilm formation of pathogens was done using Congo red agar following previous modification except for the use of 20 % glucose instead of sucrose (3.6 %) in brain heart infusion medium. After incubation, plates were scored for inhibition of brown-black color colonies in the presence of NP's and red colonies were scored as positive results while brown colonies were produced by biofilm formers in the absence of NP's.

Antibiofilm activity of NPs both coated and non-coated was determined by following protocol (Hassani et al., 2015) against plant and fish pathogens. Polystyrene coupons were added into each respective well of microtitre plate for microscopic biofilm analysis. 100 µl of 0.6mg/ml NPs were added into each respective well of sterile microtitre 96-well plate along with 100 µl of tested organisms (OD_{600}= 0.5) and erythromycin (3mg/ml) is positive control. After incubation of 48 h, normalized biofilm was calculated for quantitative estimation of biofilm inhibition and for microscopic image analysis, sterile polystyrene coupons with adhered biofilm cells were removed carefully, and observed under light microscope.

NPs and their role in plant growth promotion in the presence of phytopathogens

Coated and non-coated NP's were used for seeds germination in order to investigate their role in plant growth promotion under effect of plant pathogens. This experiment was performed using protocol of Afrasayab *et al*. (2010) with few modifications. For this purpose, wheat seeds were sterilized using 0.1 % HgCl and then coated with NP's and inoculated with plant pathogens (HT5, HT6 and HT7). Afterwards, pots were soaked with water and placed in dark for 3 days at room temperature. And then pots were transferred to light and harvesting was done after 10 days to check plant growth parameters *i.e.* germination (%), root length (cm), shoot length (cm) and seedling length (cm).

RESULTS

Antibacterial activity of bacterial EPS

EPS extracted from 10 bacterial strains were used as an antimicrobial agent against plant pathogen (HT7). EPS showed visible zones of inhibition against plant pathogen and significant ($p \leq 0.05$) maximum activity was observed at least conc. of EPS; 0.2mg/ml (Table I) and biggest zone of 32.5mm was observed by HFP (*Bacillus subtilis*) (Fig. 1).

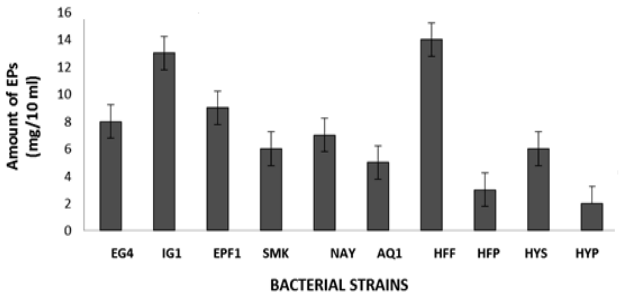

Fig. 1. Comparative quantification analysis of EPS production from different strains of Bacteria.

Table II shows results of turbidity assay. The maximum antibacterial activity of EPS was observed against isolate TM4 among all pathogens. When the extracted EPS of all strains were tested against all pathogens, it was found that maximum antibacterial activity was exhibited by EPS of strain IG1.

Comparative analysis of antimicrobial activity of EPS of all strains revealed that maximum activity against HT5 isolate was showed by strain NAY. When EPS of strain HYS was tested against pathogens, it was found that it tend to inhibit the growth of isolate HT6 and TS1 but maximum antibacterial activity was recorded against TS1 (fish pathogen) as compared to pathogenic culture significantly ($p \leq 0.05$). Similarly, significantly ($p \leq 0.05$) maximum activity of EPS of IG1 strain was recorded against HT7 and NP4 with maximum growth reduction of TM4. When EPS from EG4 strain was tested against pathogens then it was found that EG4 inhibited the growth of both HT7 and NP4 but significant ($p \leq 0.05$) reduction was recorded in case of HT7 (plant pathogen). In general, significant ($p \leq 0.05$) reduction in microbial growth was recorded by EPS of all ten strains against all pathogens as compared to bacterial culture of each pathogen (negative control= without EPS) (Table II).

Table I. Antimicrobial activity of different concentrations of exopolysaccharides (EPS) as demonstrated by zone of inhibition (mm) (Mean±SE) against plant pathogen HT7.

S. No.	Bacterial strains	Zone of inhibition (mm) at varying concentrations of EPS (Mean±SE)					
		0.2mg/ ml	0.4mg/ ml	0.6mg/ ml	0.8mg/ ml	1mg/ ml	Control erythromycin (3mg/ml)
1.	*Bacillus cereus* (EG4)	29±0.82	23.5±0.41	6.5±3.68	13±0.82	8±1.63	35.5±2.04
2.	*Citrobacter freundii* (IG-1)	24.5±1.23	14.5±2.86	15±0	7±4.09	4±0	38.5±0.41
3.	*Exigoubacterium auranticum* (EPF1)	27.5±1.23	20±0.82	12±4.09	9.5±3.68	10.5±0.41	36.5±0.41
4.	*Bacillus licheniformis* (SMK)	26.5±2.86	20.5±0.41	3.5±1.23	4.5±3.68	3.5±2.86	36±0.82
5.	*Bacillus subtilis* (NAY)	24±0	20±0.82	15.5±0.41	13.5±0.41	11.5±0.41	32±3.27
6.	*Alkaligene faecalis* (AQ-1)	32±2.45	13±5.72	12.5±3.68	14±1.63	15±4.09	41±0.82
7.	*Bacillus cereus* (HFF)	28±3.27	17.5±2.86	8.5±5.31	6.5±5.31	13±2.45	39.5±0.41
8.	*Bacillus subtilis* (HFP)	32.5±1.23	29±1.63	23±0.82	9.5±2.04	18±0	39±0.82
9.	*Bacillus subtilis* (HYS)	26±3.27	30±1.63	20.5±2.04	7.5±1.23	20.5±0.41	34±1.63
10.	*Bacillus subtilis* (HYP)	28±3.27	25±4.09	23±0	26±0.82	16.5±4.5	35.5±3.68

LSD for strains= 1.94; LSD for treatments= 3.70

Table II. Antimicrobial activity of optimized concentration of of EPS as demonstrated by bacterial growth inhibition using turbidity measurement (600 nm).

Isolates/ Media	Zone of inhibition (mm) Mean±SE						
	HT5	HT6	HT7	SCC4	NP4	TS1	TM4
LB	0.108±0.008	0.109±0.001	0.111±0.002	0.109±0.002	0.115±0.002	0.119±0.02	0.123±0.004
Control	0.987±0.004	0.728±0.009	0.408±0.001	0.317±0.001	0.296±0.001	0.254±0.01	0.266±0.009
Culture	1.457±0.002	1.998±0.005	1.556±0.009	1.945±0.008	1.363±0.009	1.34±0.007	1.194±0.005
EG4	1.08±0.03	0.97±0.04	0.813±0.01	0.94±0.002	0.904±0.002	0.86±0.01	0.779±0.01
IG1	1.065 ±0.01	0.98±0.004	0.89±0.002	0.87±0.02	0.95±0.01	0.86±0.02	0.73±0.03
EPF1	1.069±0.008	1.023±0.008	0.98±0.01	0.94±0.004	1.04±0.03	0.90±0.0004	0.86±0.02
SMK	1.11±0.007	0.996±0.007	0.82±0.01	0.937±0.009	1.05±0.01	0.91±0.003	0.798±0.03
NAY	0.999±0.04	1.01±0.008	0.97±0.04	0.98±0.02	1.07±0.02	0.89±0.05	0.86±0.01
AQ1	1.11±0.01	1.04±0.007	0.9±0.006	0.98±0.006	0.92±0.005	0.89±0.01	0.9±0.03
HFF	1.03±0.02	0.996±0.008	0.94±0.11	0.96±0.005	1.04±0.03	0.85±0.01	0.78±0.03
HFP	1.02±0.04	1.01±0.03	0.91±0.05	0.89±0.006	1.02±0.006	0.82±0.02	0.9±0.02
HYS	1.05±0.009	0.93±0.02	0.82±0.005	0.92±0.01	0.99±0.002	0.82±0.007	0.89±0.02
HYP	1.11±0.02	0.996±0.07	0.91±0.03	0.97±0.01	0.99±0.004	0.92±0.02	0.98±0.03
LSD for strains=0.24 LSD for treatments =0.14							

LSD for strain= 0.24; LSD for treatment= 0.14

Antimicrobial activity of non coated and EPS coated iron NPs

Iron NPs yield of precipitates was 1.01% (1.014g/100ml). While zinc NPs yield was 2.039% (2.039g/100ml). EPS coated iron NPs were synthesized chemically and their formation was confirmed by visual inspection of reddish brown precipitates. The yield of precipitates was 2.58% (2.58g/100ml). EPS coated zinc NPs were synthesized and white thick cloudy precipitates were formed at bottom of flask. The yield of precipitates was 2.67% (2.67g/100ml).

Table III shows that antimicrobial analysis of both

non-coated and EPS-coated iron NPs and only EPS revealed that visible zones were observed against plant pathogen (HT7). Antimicrobial activity of non-coated and EPS-coated iron NP's revealed that maximum antibacterial activity was shown by non-coated iron NP's (zone diameter= 31mm) as compared to EPS-coated iron NP's (zone diameter= 29.5 mm) at 0.8 mg/ml conc. In general, significant ($p<0.05$) activity was observed by non-coated iron NPs as compared to EPS (23.5mm). Non-coated iron NP's showed significant ($p <0.05$) antibacterial activity at 0.8 mg/ml conc. as compared to 0.2 mg/ml conc.

The antimicrobial activity analysis revealed that both coated and non-coated zinc NPs showed visible zones of inhibition against plant pathogen (HT7). Significant ($p\leq0.05$) antibacterial activity was recorded by non-coated zinc NP's with largest zone diameter (22.5 mm) at 0.6mg/ml concentration as compared to EPS-coated zinc-NP's (15.5 mm at 0.2 mg/ml conc.). In general, it was recorded that significant ($p\leq0.05$) antibacterial activity of non-coated zinc NP's was observed at 0.6mg/ml conc. as compared to 0.2 mg/ml concentration.

Table IV shows turbidity assay performed using optimized conc. of NP's (optimized conc. of iron and zinc NPs were 0.8 mg/ml and 0.6 mg/ml, respectively) in order to determine the bacteriostatic effect of NPs against both plant and fish pathogens. Comparative analysis of antibiofilm activity revealed that significant ($p\leq0.05$) maximum antibacterial activity was observed by erythromycin as compared with EPS. While activity of NP's against pathogens revealed that there was a general trend in growth inhibition and significant ($p\leq0.05$) reduction in growth was observed by NP's.

Efficacy of coated and non coated NPs in biofilm inhibition

Biofilm formation was determined by crystal violet ring formation assay. Analysis revealed that visible purple ring was observed along the sidewalls of tubes. Quantitative estimation was represented as normalized biofilm. In general, it was found that maximum biofilm formation was recorded after 24 h by isolates HT5, NP4, TS1 and TM4. While isolate HT6 tend to produce maximum biofilm after 48 h of incubation. HT7 and SCC4 isolates produce pronounced biofilm after 72 h.

Table III. Antimicrobial activity of varying concentrations of non-coated and coated NPs, EPS and erythromycin as demonstrated by zone of inhibition (mm) against plant pathogen.

S. No	Treatment	Zone of inhibition (mm) at varying conc. of NP's (Mean±SE)				
		0.2mg/ml	0.4mg/ml	0.6mg/ml	(0.8mg/ml)	1mg/ml
1.	Iron	10±0.82	30.5±1.23	30.5±0.41	31±0.82	24±0.82
2.	Iron-EPS	5±0.82	26±0.82	29.5±0.41	28.5±2.04	22±0.82
3.	EPS	3±0.82	23.5±0.41	22.5±2.04	19.5±0.41	18±0.82
4.	Zinc	2±2.45	18.5±2.04	22.5±1.23	21±0.82	13±1.63
5.	Zinc-EPS	15.5±1.23	8.5±2.04	8.5±0.41	7±0.82	11±0.82
6.	Erythromycin	39±0.82	43±0.82	41.5±0.41	40.5±0.41	43.5±0.41

LSD for strain= 6.47; LSD for treatment= 7.08

Table IV. Antimicrobial activity of NP's against pathogens by turbidity analysis at 600 nm.

Isolates	Turbidity assay of NPs (OD_{600}) (Mean±SE)							
	LB media	Pure culture	Zinc	Zinc-EPS	Fe	Fe-EPS	EPS	Erythromycin
Plant pathogens								
HT5	0.108±0.0008	1.817±0.07	0.96±0.02	0.86±0.01	1.11±0.02	1.114±0.005	1.081±0.03	0.881±0.04
HT6	0.109±0.001	2.011±0.05	0.75±0.03	0.84±0.006	0.96±0.02	1.02±0.002	1.075±0.05	1.052±0.02
HT7	0.111±0.002	1.796±0.001	0.77±0.007	0.91±0.04	1±0.04	0.87±0.04	1.204±0.06	0.51±0.07
Fish pathogens								
SCC4	0.109±0.002	1.997±0.001	0.92±0.009	0.99±0.04	1.04±0.03	1.05±0.05	0.946±0.01	0.394±0.02
NP4	0.115±0.002	1.857±0.001	0.84±0.01	0.93±0.06	0.84±0.04	1.06±0.006	0.987±0.02	0.373±0.01
TS1	0.119±0.02	1.806±0.01	0.79±0.001	0.86±0.02	0.96±0.008	0.99±0.02	0.923±0.1	0.357±0.03
TM4	0.123±0.01	1.836±0.009	0.7±0.006	0.71±0.008	0.92±0.05	0.96±0.06	1.292±0.06	0.32±0.02

LSD for strain= 0.14; LSD for treatment= 0.134

Table V. Antibiofilm activity of EPS-Coated and Non-Coated NP's against biofilm formation by pathogens.

Isolates	Culture	Zinc	Zinc-EPS	Fe	Fe-EPS	EPS (HFP)	Ery
HT5	0.46606842	0.66170213	0.83333333	0.62385321	0.66666667	0.81429898	0.35187287
HT6	0.61177078	0.75675676	1.1547619	1.04166667	0.86407767	0.85154062	0.7992278
HT7	0.73348018	0.98734177	0.88043478	0.71287129	0.74712644	0.32971619	0.64646465
SCC4	0.50928793	0.98913043	0.67676768	1.18446602	0.90291262	0.51175214	1.3562341
NP4	0.57831978	0.6746988	1.03333333	1.24096386	0.73076923	0.71179487	2.82786885
TS1	0.55069124	1.64935065	1.23809524	1.06521739	0.75257732	0.52802691	2
TM4	0.59457995	0.76811594	1.43478261	1.02197802	0.59139785	0.4331761	1.73088685

LSD for strain= 0.4; LSD for treatment= 0.4

Results revealed that light brown-brown black colored colonies were observed on negative control plates while plates supplemented with NPs, effectively inhibited biofilm formation ability of pathogens and light red colored colonies were observed on BHI agar plates (Supplementary Fig. S1).

Effects of EPS-coated and non-coated NPs against biofilms of fish pathogens

Antibiofilm assay was performed for EPS-coated and non-coated using optimized conc. of NP's (0.6mg/ml) against plant (HT5, HT6 and HT7) and fish (SCC4, NP4, TS1 and TM4) pathogens. Analysis of antibiofilm activity revealed that significant ($p \leq 0.05$) biofilm inhibition was observed by EPS as compared to erythromycin. While antibiofilm activity of NP's against pathogens revealed that there was a general trend in biofilm inhibition and significant ($p \leq 0.05$) reduction in biofilm formation was observed by non-coated zinc NP's as compared to other NP's (Table V). Antibiofilm activity vary with each pathogen but there was a general trend in biofilm inhibition and significant reduction in biofilm was recorded by both EPS-coated iron and non-coated zinc NPs as shown in Table V.

Transparent plastic coupons were used for biofilm development. Microscopic image analysis revealed that thick clumps of biofilm were produced due to increased incubation time (Supplementary Fig. S2, Label=W, Y, T) thus, bacterial aggregates were developed indicating the presence of biofilm. Partial inhibition of biofilm was observed as minor clumps (Supplementary Fig. S2, Label= H, I, J) and it was mostly observed when NPs were used during biofilm development. There was a general trend of increased biofilm with time of incubation and thick clumps were observed in microscope. However, biofilm inhibition was clearly seen in presence of EPS as shown in image (Supplementary Fig. S2) label coupon A=11A indicates the biofilm inhibition of pathogen HT5. Microscopic image analysis E revealed the biofilm inhibition of NP4 pathogen by EPS-coated iron NP's. Visible clumps of TS1 pathogen were observed in image F after treatment with EPS-coated iron NP's indicate the partial inhibition of biofilm (Supplementary Fig. S2). However, there was a general trend and microscopic image analysis revealed that results of antibiofilm activity were in line with results presented in Table V.

Effects of NPs in inhibiting growth of phytopathogens

Figure 2 shows that plant germination was determined in the presence of both coated and non-coated zinc and iron NPs and %germination was recorded.

Effects of NPs on plant growth promotion

Plant germination was recorded in the presence of plant pathogens (HT5, HT6 and HT7) and it was observed that there was a general trend of decrease in seeds germination as compared to control plants without pathogens inoculum (Fig. 2). However, Percentage germination was more in the presence of HT5 only as compared to HT5 and EPS coated Zn NPs.

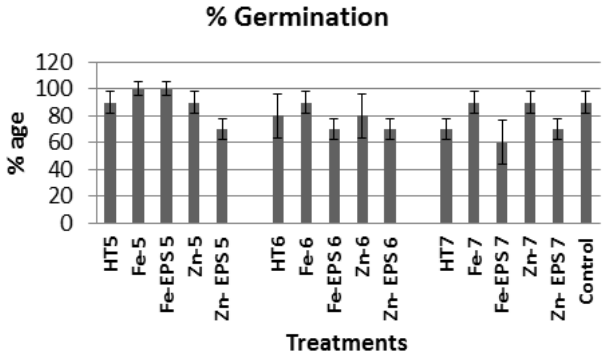

Fig. 2. Germination (%) of wheat seeds in the presence and absence of plant pathogens.

Table VI shows the efficacy of both coated and non-coated iron and zinc NPs was determined on plant roots length, it was observed that plant roots treated with NPs

were effectively increased. In general, significant ($p \leq 0.05$) increment in root growth was observed in presence of both EPS-coated iron and zinc NPs along with presence of plant pathogens (Table VI).

When shoot lengths of coated and non-coated NPs were determined, it was recorded that shoot length was effectively improved in presence of NPs and in general it was observed that shoot length was significantly ($p \leq 0.05$) increased in presence of EPS-coated zinc NP's instead in the presence of phytopathogens (Table VI).

Effect of NPs was checked on seedling length in presence of plant pathogens and it was recorded that seedling length was significantly ($p \leq 0.05$) improved in the presence of NPs. There was a general trend of plant length improvement and it was observed that seedling length was effectively improved in presence of EPS-coated zinc NPs as compared to control non-treated plants (Table VI).

Table VI. Plant length parameters of wheat seedlings after treatment with NPs under effect of plant pathogens HT5, HT6 and HT7.

Treatment	Plant lengths (cm) (Mean±SE)		
	Root	Shoot	Seedling
HT5	3.2±0.08	10.37±0.44	13.57±0.53
Fe-5	3.38±0.11	8.49±0.04	11.87±0.07
Fe-EPS 5	2.88±0.13	8.73±0.67	11.61±0.54
Zn-5	2.52±0.18	6.88±0.62	9.4±0.43
Zn- EPS 5	3.5±0.04	10.38±0.33	13.9±0.38
HT6	3.4±0.14	8.39±0.44	11.79±0.59
Fe-6	3.27±0.55	8.17±0.59	11.44±1.14
Fe-EPS 6	3.89±0.06	9.33±0.25	13.23±0.31
Zn-6	3.37±0.52	9.23±0.6	12.59±1.12
Zn- EPS 6	2.72±0.07	9.97±2.04	12.7±1.96
HT7	2.85±0.15	8.36±0.47	11.21±0.62
Fe-7	2.78±0.04	9.36±0.70	12.14±0.65
Fe-EPS 7	2.76±0.45	8.02±1.24	10.78±1.70
Zn-7	3.61±0.15	8.61±0.69	12.23±0.84
Zn- EPS 7	3.52±0.12	7.89±0.94	11.41±0.82
H2O	2.76±0.23	7.35±0.36	10.11±0.13

LSD for strain=0.42; LSD for Treatment= 0.96

DISCUSSION

Antibacterial resistance is major problem because of excessive and uncontrolled usage of antimicrobial agents and hence, to overcome this problem, antimicrobial agents *i.e,* EPS and chemically synthesized NP's conjugated with EPS, were exploited against plant and fish pathogens in order to determine their efficacy to inhibit their growth. Furthermore, effect of NPs was also determined in plants for seeds germination in presence of pathogens under effect of NPs.

EPS was synthesized, extracted and quantified from bacterial strains *Bacillus cereus* (EG4), *Citrobacter freundii* (IG-1), *Exigoubacterium auranticum* (EPF1), *Bacillus cereus* (HFF), *Bacillus subtilis* (HFP), *Bacillus subtilis* (HYP), *Bacillus subtilis* (HYS), *Bacillus licheniformis* (SMK), *Alkaligene faecalis* (AQ-1), *Bacillus subtilis* (NAY) using LB-broth medium. Antimicrobial activity (MIC) of EPS of all strains was determined and MIC value was recorded as 0.2mg/ml conc. Similar results were observed (Li *et al*., 2014) that EPS extracted from *Bifidobacterium bifidum* WBIN03 and *Lactobacillus plantarum* R315 exhibit antibacterial activity against pathogens including *Cronobacter sakazakii, Escherichia coli, Listeria monocytogenes, Staphyloccocus aureus, Candida albicans, Bacillus cereus, Salmonella typhimurium*, and *Shigella sonnei* at 300 µg/ml conc. Li *et al*. (2014). Antimicrobial analysis of EPS was determined against pathogens using microtitre turbidity assay and visible reduction in culture turbidity was recorded (Wang et al., 2015) also found that the EPS produced by *Lactobacillus plantarum* YW32 exhibited a concentration dependent inhibitory effect on the formation of biofilms by several pathogenic bacteria, including *Escherichia coli* O157, *Shigella flexneri* CMCC (B), *Staphylococcus aureus* AC1 and *Salmonella typhimurium* S50333.

NPs are of great importance now a days and researchers are in struggle to synthesize different NPs using metal oxides (gold, zinc, platinum, silver, and palladium) (Malaikozhundan *et al*., 2016). To determine antimicrobial activity of NPs, iron and zinc NPs were synthesized using chemicals and plants extracts (green tea and aloevera, respectively). Both iron and zinc NP's were conjugated with bacterial EPS and both coated and non-coated iron and zinc NPs were used to check their effect on microbial growth and both coated and non coated NP's were characterized by XRD and SEM analysis.

ZnO NPs were characterized by XRD analysis using XRD diffractometer for 2θ values using CuKα radiation at λ = 1.54056Å and analysis revealed the value of 2θ as 31.5°(100), 36°(101), 47°(102), and 62.5°(103). Similar findings were also reported by Varghese and George, 2015 when they synthesized ZnO NP's from aloevera extract, thus their findings and 2θ values supporting our findings (Varghese and George, 2015). The XRD spectrum revealed the hexagonal structure of synthesized ZnNPs. SEM analysis of ZnO NP's revealed the crystalline structure and NPs were found to be needle like hexagonal centro-

symmetric structures. Particles were found to be present within size range of 80-200 nm in diameter.

Iron NPs were synthesized by green synthesis using green tea leaves extract and were brown-black in color. Similar results were reported in the previous findings (Markova et al., 2012; Gottimukkala *et al*., 2017). The characterization of obtained NP's was done through SEM analysis and XRD. SEM analysis revealed that synthesized NPs were centro-symmetric crystalline structures with cubic morphology and size ranges from 200-700nm. Spepctrum analysis revealed that 2θ values 33°, 43°, 55° and 64°were observed revealing the planes as 311, 400, 511 and 440, respectively. XRD spectrum analysis was supported by findings diffraction of planes was recorded as 2θ values 30° (220), 33° (311), 43° (400), 53° (422), 55° (511), 64° (440) and 90° (731) .

EPS-coated iron NPs were synthesized chemically and characterization of NPs by SEM revealed that spherical NPs were present with large aggregates due to presence of EPS and size of NPs was observed ranging from 200-800nm (Supplementary Fig. S3). XRD spectrum analysis revealed that different peaks were observed 35.5°(311), 43°(400) (Supplementary Fig. S4). Results were justified by finding reported (Varghese and George, 2015) they synthesized EPS-coated iron NPs and revealed that 2θ values were observed at different planes of nanostructures including (311), (400) and (511), respectively (Varghese and George, 2015).

EPS-coated zinc NPs were synthesized and characterized by SEM and XRD spectrum analysis. SEM imaging revealed that NP's appeared like aggregates of needles and film like structures and their diameter was recorded and NP's were in size ranging from 200-500nm in diameter. XRD analysis and diffraction was recorded at different angles recorded as 31.5°, 47° and 69° revealing diffraction from planes (100), (102) and (201), respectively. Similar analysis of EPS-coated zinc NP's was reported (Abinaya *et al*., 2018) that 2θ values obtained from XRD analysis of EPS-coated zinc NP's were recorded as 31.67°, 34.31°, 47.40°, 56.52°, 62.73°, 67.91°and 69.03° which correspond to lattice planes of crystalline structure 100, 002, 102, 110, 103, 112 and 201 thus reporting the synthesis of pure structure of EPS-coated ZnONPs (Abinaya *et al*., 2018).

Antimicrobial potential of ZnO NPs was determined against plant pathogen and maximum antibacterial activity was recorded at 0.6mg/ml conc. and zone diameter was recorded 22.5 mm. Similar results were observed (Farzana *et al*., 2017) that zone size (23mm) recorded as antimicrobial effect of zinc NP's against pathogenic bacteria, *K. pneumoniae* 2 strain at 0.6mg/ml conc. Farzana *et al*. (2017). Antimicrobial activity of ZnO NPs was determined and revealed that maximum growth inhibition was observed against *P. aeruginosa* at maximum conc. and zone diameter was recorded as 22 mm.

Antimicrobial activity of iron NPs revealed that maximum antibacterial activity was observed at 0.8mg/m and zone size recorded was 31 mm against phytopathogen. It was reported that maximum activity of iron NP's was observed at highest conc. against *K. pneumoniae* and *Bacillus cereus* and zone size was recorded as 26 mm and 22 mm, respectively (Ansari *et al*., 2014).

EPS-coated iron NPs were used against plant pathogen (HT7) and maximum zone diameter was recorded as 29.5mm. It was revealed that maximum activity of NPs was observed at 0.4mg/ml conc. and zone size was recorded as 7.66mm against strain of *A. hydrophila* (ATCC 49140) (Varghese and George, 2015).

EPS-coated zinc NPs were synthesized and their antibacterial activity was observed against HT7 and it was found that maximum activity was shown at 0.2mg/ml conc. of zinc NPs and zone size was recorded as 15.5mm. These results were in line with observations (Abinaya *et al*., 2018), when antibacterial activity of EPS-coated ZnO NPs was determined against gram positive bacteria using agar well diffusion method and revealed that maximum zone size recorded was 10.2mm at 0.1mg/ml conc (Abinaya *et al*., 2018).

Antimicrobial assay was performed using microtitre turbidity assay and results revealed that visible reduction was observed in turbidity of pathogenic isolates and maximum antibacterial activity was recorded by non-coated iron NPs as compared to coated ones. It was reported that iron NPs are effective antibacterial agents and significant reduction in bacterial growth was recorded with increasing conc. of NPs while bacterial growth was completely inhibited at maximum conc. 3mg/ml).

Antibacterial activity of zinc oxide NPs by turbidity assay revealed that maximum growth inhibition was recorded by non-coated zinc oxide NPs as compared to EPS-coated zinc NPs. Hassani *et al*. (2015) it was revealed that zinc oxide NPs are highly effective antimicrobial agents and they resulted in 94% OD reduction (*P. aeruginosa*) in wells of microtitre treated with maximum conc. 350µg/ml) of zinc NPs (Hassani *et al*., 2015).

Qualitative test for biofilm formation of pathogens was performed by ring and tubes were observed for appearance of a visible purple colored ring on the side walls and the tube bottom. Different pathogens form violet ring of biofilm with varying color intensity depending upon time of incubation. Similar results were observed (Liaqat *et al*., 2021) that biofilm formation of *Staphylococcus sciuri* (HP3) was observed in presence of varying conc. of NaCl and revealed that violet ring was formed with varying

thickness of ring with increased time of incubation (Liaqat *et al*., 2021). For quantitative estimation of biofilm, results were represented in form of normalized biofilm (OD_{570} / OD_{600}) because there was different trend in culture growth and biofilm formation. The normalization of biofilm has been reported to be helpful and clearly present a data set of biofilm formation for the conditions when growth is limited.

Qualitative analysis for biofilm formation and its inhibition was tested by congo red assay in which Brain Heart Infusion agar was used and 3.6% sucrose (Liaqat *et al*., 2023). Following the protocol, colonies that appear on BHIC plates vary in color and they can be differentiated between biofilm formers and non-formers due to presence or absence of brown color after incubation (Liberto *et al*., 2009). Plates were observed after incubation and the colony color was recorded as light brown colored colonies on control plates without NP's and the appearance of brown-black colonies after 24-48 h of culture incubation indicates that these bacteria are biofilm producers (Arciola *et al*., 2002). While plates supplemented with NPs shows different pattern of colony color because in the presence of NPs, biofilm forming ability of pathogens was compromised and they were unable to produce biofilm their colony color was varying from light to bright red colored colonies on BHI agar plates. Similar trend was observed when they performed qualitative assay of biofilm inhibition of *Candida* sp. and observed that biofilm formation and cell growth was suppressed by silver NPs (Jalal *et al*., 2019).

Antibiofilm activity of both EPS-coated and non-coated iron and zinc NPs was determined against plant and fish pathogens using Microtitre turbidity assay and significant reduction in biofilm formation was reported. Maximum antibiofilm activity was reported by non-coated zinc NPs as compared to other NP's that resulted in maximum inhibition of biofilm formation of pathogens at high conc (0.6mg/ml). Similar observations of biofilm inhibition were also reported (Hassani *et al*., 2015) that zinc oxide NPs are highly effective at inhibiting biofilm formation of pathogenic isolates of *Pseudomonas aeruginosa* and inhibition was recorded at maximum conc. of Zinc oxide NPs (Hassani *et al*., 2015).

Biofilm inhibition was also observed by both EPS coated and non-coated iron NPs and it was concluded that EPS-coated iron NPs significantly reduce biofilm formation of pathogens as compared to non-coated (Iconaru *et al*., 2012) reported that iron oxide glycerol NPs (GIO-NP's) effectively inhibit the biofilm formation of both gram positive (*E. faecalis*) and gram negative (*P. aeruginosa*) at increasing conc. of NPs (Iconaru *et al*., 2012).

Iron NPs have multiple agricultural applications as fertilisers, pesticides or growth stimulators as reported previously (Aleksandrowicz-Trzcińska *et al*., 2019). Effect of both EPS coated and non-coated iron and zinc NPs was determined on plant growth in presence of plant pathogens. Results of plant growth promotion revealed that plant growth was significantly improved in presence of iron NPs. Hence NPs also tend to improve plant growth by inhibiting growth of pathogens as well reported that plant growth was significantly improved at 0.05mM/l conc. of iron NPs and maximum plant height was recorded at that conc. as compared to negative control (without NPs). When effect of zinc NPs was determined on plant growth then it was concluded that maximum plant growth promotion was recorded by EPS-coated zinc NPs as compared to non-coated in presence of plant pathogens. Previously, it was reported that plant growth of wheat was significantly improved in presence of zinc NPs even zinc content of plants was significantly improved in presence of zinc NP's as compared to non-treated plants. Lengths of root shoot and seedlings is lesser in case of water only than those in the presence of any one of all plant pathogens, this might be some initial positive interactions in terms of exchange of exudates that seems to improve plant growth but further experiments with different plants and different life stages of plants yet to be explored.

CONCLUSIONS

The research conducted thus indicated the efficacy of antimicrobial and antibiofilm effect of EPS and both EPS coated and non-coated iron and zinc NPs on the phyto pathogens and fish pathogens as well. Initially, EPS producing strains were exploited for production of EPS followed by antimicrobial activity. Biofilm production of pathogens was analyzed qualitatively along with antibacterial and antibiofilm activity of EPS and both EPS coated and non-coated iron and zinc NPs using Kirby Bauer disc diffusion method, microtiter assay for turbidity and biofilm inhibition as well as microscopic biofilm analysis. The study concluded that both NPs and EPS were proved to be effective antibacterial and antibiofilm agents against both plant and fish pathogens. Furthermore, both EPS coated and non-coated NPs were found to be effective plant growth promoters by inhibiting growth of plant pathogens. The antibiofilm profile of NPs and their interaction with plants and phytopathogens have indicated that they can be used as effective alternative of antimicrobial agents against plant and fish pathogens, and drug resistant strains of biofilm formers and as plant growth promoting and seed sterilizing agents as well in agricultural field showing a promising approach in

nanotechnology and plant sciences.

DECLARATIONS

Acknowledgement

This research work is from MPhil thesis of Sana Yousaf who completed her research at Garrison University, Lahore.

Supplementary material

There is supplementary material associated with this article. Access the material online at: https://dx.doi.org/10.17582/journal.pjz/20240619130642

Statement of conflict of interest

The authors have declared no conflict of interest.

REFERENCES

Abinaya, M., Vaseeharan, B., Divya, M., Sharmili, A., Govindarajan, M., Alharbi, N.S. and Benelli, G., 2018. Bacterial exopolysaccharide (EPS)-coated ZnO nanoparticles showed high antibiofilm activity and larvicidal toxicity against malaria and Zika virus vectors. *J. Trace Elem. Med. Biol.*, **45**: 93-103. https://doi.org/10.1016/j.jtemb.2017.10.002

Afrasayab, S., Faisal, M. and Hasnain, S., 2010. Comparative study of wild and transformed salt tolerant bacterial strains on *Triticum aestivum* growth under salt stress. *Braz. J. Microbiol.*, **41**: 946-955. https://doi.org/10.1590/S1517-83822010000400013

Aleksandrowicz-Trzcińska, M., Bederska-Błaszczyk, M., Szaniawski, A., Olchowik, J. and Studnicki, M., 2019. The effects of copper and silver nanoparticles on container-grown Scots pine (*Pinus sylvestris* L.) and pedunculate oak (*Quercus robur* L.) seedlings. *Forests*, **10**: 269. https://doi.org/10.3390/f10030269

Allaker, R.P. and Memarzadeh, K., 2014. Nanoparticles and the control of oral infections. *Int. J. Antimicrob. Agents*, **43**: 95-104. https://doi.org/10.1016/j.ijantimicag.2013.11.002

Ansari, M.A., Khan, H.M., Khan, A.A., Cameotra, S.S. and Pal, R., 2014. Antibiofilm efficacy of silver nanoparticles against biofilm of extended spectrum β-lactamase isolates of *Escherichia coli* and *Klebsiella pneumoniae*. *Appl. Nanosci.*, **4**: 859-868. https://doi.org/10.1007/s13204-013-0266-1

Aqsa, Qurashi, A.W. and Moqaddes, S., 2023. Microbial bio-film calcite mediated removal of heavy metals from industrial wastewater of Kasur, Pakistan. *J. Basic Microbiol.*, **63**: 986-995. https://doi.org/10.1002/jobm.202300232

Arciola, C.R., Campoccia, D., Gamberini, S., Cervellati, M., Donati, E. and Montanaro, L., 2002. Detection of slime production by means of an optimized Congo red agar plate test based on a colorimetric scale in Staphylococcus epidermidis clinical isolates genotyped for *Ica locus*. *Biomaterials*, **23**: 4233-4239. https://doi.org/10.1016/S0142-9612(02)00171-0

Baelo, A., Levato, R., Julián, E., Crespo, A., Astola, J., Gavaldà, J. and Torrents, E., 2015. Disassembling bacterial extracellular matrix with DNase-coated nanoparticles to enhance antibiotic delivery in biofilm infections. *J. Contr. Release*, **209**: 150-158. https://doi.org/10.1016/j.jconrel.2015.04.028

Banik, S. and Luque, A.P., 2017. *In vitro* effects of copper nanoparticles on plant pathogens, beneficial microbes and crop plants. *Span. J. agric. Res.*, **15**: 23. https://doi.org/10.5424/sjar/2017152-10305

Bauer, A.W., Kirby, W.M.M., Sherris, J.C. and Turck, M., 1966. Antibiotic susceptibility testing by a standardized single disk method. *Am. J. clin. Pathol.*, **45**: 493-496. https://doi.org/10.1093/ajcp/45.4_ts.493

Bhattacharya, P. and Neogi, S., 2017. Gentamicin coated iron oxide nanoparticles as novel antibacterial agents. *Mater. Res. Express*, **4**: 095005. https://doi.org/10.1088/2053-1591/aa8652

Castellane, T.C.L., Lemos, M.V.F. and de Macedo Lemos, E.G., 2014. Evaluation of the biotechnological potential of *Rhizobium tropici* strains for exopolysaccharide production. *Carbohydr. Polym.*, **111**: 191-197. https://doi.org/10.1016/j.carbpol.2014.04.066

Chen, T. and Nan, Z., 2015. Effects of phytopathogens on plant community dynamics: A review. *Acta Ecol. Sin.*, **35**: 177-183. https://doi.org/10.1016/j.chnaes.2015.09.003

Ciofu, O., Rojo-Molinero, E., Macià, M.D. and Oliver, A., 2017. Antibiotic treatment of biofilm infections. *Apmis*, **125**: 304-319. https://doi.org/10.1111/apm.12673

CLSI Chart (Clinical and Laboratory Standards Institute), 2018. Performance standards for antimicrobial susceptibility testing (28th ed.). CLSI supplement M100.

Farzana, R., Iqra, P., Shafaq, F., Sumaira, S., Zakia, K., Hunaiza, T. and Husna, M., 2017. Antimicrobial behavior of zinc oxide nanoparticles and β-lactam antibiotics against pathogenic bacteria. *Arch. clin.*

Microbiol., **8**: 57. https://doi.org/10.4172/1989-8436.100057

Ferreira, A.A., Tette, P.A.S., Mendonça, R.C.S., Soares, A.D.S. and Carvalho, M.M.D., 2014. Detection of exopolysaccharide production and biofilm-related genes in *Staphylococcus* spp. isolated from a poultry processing plant. *Fd. Sci. Technol. Campinas*, **34**: 710-716. https://doi.org/10.1590/1678-457X.6446

Fujishige, N.A., Kapadia, N.N., De Hoff, P.L. and Hirsch, A.M., 2006. Investigations of Rhizobium biofilm formation. *FEMS Microbiol. Ecol*., **56**: 195-206. https://doi.org/10.1111/j.1574-6941.2005.00044.x

Ghalem, B.R., 2017. Antioxidant and antimicrobial activities of exopolysaccharides from yoghurt starter. *Am. J. Chem. Biochem. Eng*., **2**: 35-39.

Gottimukkala, K.S.V., Harika, R.P. and Zamare, D., 2017. Green synthesis of iron nanoparticles using green tea leaves extract. *J. Nanomed. Biother. Discov*., **7**: 151.

Hassani, S.M., Nakhaei, M.M. and Forghanifard, M.M., 2015. Inhibitory effect of zinc oxide nanoparticles on *Pseudomonas aeruginosa* biofilm formation. *Nanomed. J*., **2**: 121-128.

Iconaru, S.L., Prodan, A.M., Le Coustumer, P. and Predoi, D., 2012. Synthesis and antibacterial and antibiofilm activity of iron oxide glycerol nanoparticles obtained by coprecipitation method. *J. Chem*., **2013**. https://doi.org/10.1155/2013/412079

Jalal, M., Ansari, M.A., Alzohairy, M.A., Ali, S.G., Khan, H.M., Almatroudi, A. and Siddiqui, M.I., 2019. Anticandidal activity of biosynthesized silver nanoparticles: Effect on growth, cell morphology, and key virulence attributes of *Candida* species. *Int. J. Nanomed*., **14**: 4667. https://doi.org/10.2147/IJN.S210449

Li, S., Huang, R., Shah, N.P., Tao, X., Xiong, Y. and Wei, H., 2014. Antioxidant and antibacterial activities of exopolysaccharides from *Bifidobacterium bifidum* WBIN03 and *Lactobacillus plantarum* R315. *J. Dairy Sci*., **97**: 7334-7343. https://doi.org/10.3168/jds.2014-7912

Liaqat, I., Khalid, A., Rubab, S., Rashid, F., Latif, A.A., Naseem, S., Bibi, A., Khan, B.N., Ansar, W., Javed, A. and Afzaal, M., 2023. *In vitro* biofilm-mediated biodegradation of pesticides and dye-contaminated effluents using bacterial biofilms. *Microorganisms*, **11**: 2163. https://doi.org/10.3390/microorganisms11092163

Liaqat, I., Mirza, S.A., Sajjad, S., Ali, S., Qamar, M.F. and Ul Haq, I., 2021. FliI role in flagellar assembly of *Salmonella* ΔfliI mutant strain determines motility and biofilm formation. *Pakistan J. Zool*., **53**: 2381-2387. https://doi.org/10.17582/journal.pjz/20190628120649

Liberto, M.C., Matera, G., Quirino, A., Lamberti, A.G., Capicotto, R., Puccio, R. and Foca, A., 2009. Phenotypic and genotypic evaluation of slime production by conventional and molecular microbiological techniques. *Microbiol. Res*., **164**: 522-528. https://doi.org/10.1016/j.micres.2007.04.004

Lourenço, F.R. and Pinto, T.D.J.A., 2011. Antibiotic microbial assay using kinetic-reading microplate system. *Braz. J. Pharm. Sci*., **47**: 573-584. https://doi.org/10.1590/S1984-82502011000300015

Mah, T.F.C. and O'toole, G.A., 2001. Mechanisms of biofilm resistance to antimicrobial agents. *Trends Microbiol*., **9**: 34-39. https://doi.org/10.1016/S0966-842X(00)01913-2

Malaikozhundan, B., Vaseeharan, B., Vijayakumar, S., Sudhakaran, R., Gobi, N. and Shanthini, G., 2016. Antibacterial and antibiofilm assessment of Momordica charantia fruit extract coated silver nanoparticle. *Biocatal. Agric. Biotechnol*., **8**: 189-196. https://doi.org/10.1016/j.bcab.2016.09.007

Markova, Z., Novak, P., Kaslik, J., Plachtova, P., Brazdova, S., Jancula, D. and Marsalek, B., 2012. Synthesis and characterization of ZnO nanoparticles for bio-application. *Chem. Pap*., **66**: 1014-1019.

Menazea, A.A. and Ismail, A.M., 2020. Novel green synthesis of zinc oxide nanoparticles using orange waste and its thermal and antibacterial activity. *RSC Adv.*, **10**: 23817–23827. https://doi.org/10.1039/D0RA04926C

Middleton, S.R., Yang, Y. and Shao, X., 2019. Optimizing Fe3O4 nanoparticle fabrication for biomedical applications: Size, shape, and surface properties. *Front. Pharmacol*., **10**: 1371.

Mishra, V. and Sharma, R., 2015. Green synthesis of zinc oxide nanoparticles using fresh peels extract of *Punica granatum* and its antimicrobial activities. *Int. J. Pharm. Sci. Res*., **6**: 2302-2312.

Mittal, D., Kaur, G. and Singh, P., 2021. Synthesis of iron oxide nanoparticles using iron-accumulating bacterium and their application as antimicrobial agent. *IET Nanobiotechnol*., **15**: 46-51.

Naseem, T. and Farrukh, M.A., 2015. Antibacterial activity of green synthesis of iron nanoparticles using *Lawsonia inermis* and *Gardenia jasminoides* leaves extract. *J. Chem.,* 2015, Article ID 912342. https://doi.org/10.1155/2015/912342

Nasrin, S. and Nesa, J., 2017. Effect of zinc oxide nanoparticles synthesized by Aloe vera on biochemical and antioxidant defense system in

Labeo rohita. *Fish. Physiol. Biochem*., **43**: 1333-1343.

Nehra, P., Chauhan, R.P., Garg, N. and Gopal, M., 2019. Antibacterial and antifungal activity of copper oxide nanoparticles against gram-positive, gram-negative bacteria and fungi. *J. Nanosci. Nanotechnol*., **19**: 4897-4907.

Panacek, A., Kolar, M., Vecerova, R., Prucek, R., Soukupova, J., Krystof, V. and Zboril, R., 2009. Antifungal activity of silver nanoparticles against *Candida* spp. *Biomaterials*, **30**: 6333-6340. https://doi.org/10.1016/j.biomaterials.2009.07.065

Pedrosa, F., Bassani, L. and Henriques, A., 2018. Antimicrobial activity of silver nanoparticles synthesized with two new tropical vegetal sources. *J. Med. Plants Res*., **12**: 220-228.

Phanjom, P. and Ahmed, G., 2017. Green synthesis of gold nanoparticles using leaf extract of Rhododendron arboreum and study of their antimicrobial activity. *J. Pharm. Res. Int*., **20**: 1-9.

Raaman, N., Rajitha, N., Jayshree, A. and Jegadeesh, R., 2013. Antimicrobial activity of silver nanoparticles synthesized from aqueous leaf extracts of *Ocimum sanctum* L. and *Solanum trilobatum* L. against bacterial pathogens. *Appl. Nanosci*., **3**: 495-500.

Qurashi, A.W. and Sabri, A.N., 2016. Induction of osmotolerance by Staphylococcus sciuri HP3 in Lens esculenta var. Masoor 93 under NaCl stress. *Pak. J. Life Soc. Sci.,* **14**: 42-51.

Rather, M.A., Sharma, R. and Aklakur, M., 2011. Synthesis and characterization of silver nanoparticles using leaf extract of *Azadirachta indica*. *Int. J. Green Nanotechnol. Biomed*., **3**: 345-354.

Ribeiro, N., Soares, G.C. and Sobral, R., 2015. Potential of selenium nanoparticles to control *Candida* spp. biofilms. *Biofouling*, **31**: 639-648.

Salman, J.A., Mohammed, F., Raghad, A.A. and Inas, A.S., 2015. Antibiofilm effect of iron oxide nanoparticles synthesized by lactobacillus fermentum on catheter. *World J. Pharmac. Res*., **4**: 317-328.

Sharma, D. and Kanchi, S., 2016. Phytosynthesis of ZnO nanoparticles using leaves extract of *Azadirachta indica* and their antibacterial activity. *J. Alloys Compd*., **688**: 712-717.

Slavin, Y.N., Asnis, J., Häfeli, U.O. and Bach, H., 2017. Metal nanoparticles: Understanding the mechanisms behind antibacterial activity. *J. Nanobiotechnol*., **15**: 1-20. https://doi.org/10.1186/s12951-017-0308-z

Swain, P., Nayak, S.K., Sasmal, A., Behera, T., Barik, S.K., Swain, S.K. and Jayasankar, P., 2014. Antimicrobial activity of metal based nanoparticles against microbes associated with diseases in aquaculture. *World J. Microbiol. Biotechnol.,* **30**: 2491-2502.

Tang, S. and Zheng, J., 2018. Antibacterial activity of silver nanoparticles: Structural effects. *Adv. Healthc. Mater*., **7**: 1701503. https://doi.org/10.1002/adhm.201701503

Varghese, E. and George, M., 2015. Green synthesis of zinc oxide nanoparticles. *Int. J. Adv. Res. Sci. Eng.,* **4**: 307-314.

Vazquez-Muñoz, R., Avalos-Borja, M., Castro-Longoria, E. and Díaz, D., 2014. Synergistic antibacterial mechanism of the silver nanoparticles with antibiotics supported by an *in situ* generation of silver ions in *Escherichia coli* and *Staphylococcus aureus*. *PLoS One*, **9**: e94405. https://doi.org/10.1371/journal.pone.0108876

Vimbela, G.V., Ngo, S.M., Fraze, C., Yang, L. and Stout, D.A., 2017. Antibacterial properties and toxicity from metallic nanomaterials. *Int. J. Nanomed*., **12**: 3941. https://doi.org/10.2147/IJN.S134526

Wang, L. and Hu, C., 2017. Copper oxide nanoparticles enhance *Pseudomonas chlororaphis* O6-induced systemic resistance to Tobacco mosaic virus. *ACS Appl. Mater. Interf*., **9**: 5275-5285.

Wang, J., Zhao, X., Tian, Z., He, C., Yang, Y. and Yang, Z., 2015. Isolation and characterization of exopolysaccharide-producing *Lactobacillus plantarum* SKT109 from Tibet Kefir. *Polish J. Food Nutri. Sci.,* **65**: 269-280.

Whiteley, C.G. and Lee, D.J., 2006. Enzyme technology and biological remediation. *Enzyme Microb. Technol*., **38**: 291-316. https://doi.org/10.1016/j.enzmictec.2005.10.010

World Health Organization, 2019. *Antimicrobial resistance: Global report on surveillance*. WHO, Geneva.

Yeo, H.C. and Lim, C.S., 2020. Antimicrobial effects of zinc oxide nanoparticles on Escherichia coli and *Staphylococcus aureus*: A mechanism study. *Appl. Microbiol. Biotechnol*., **104**: 709-720.

Zhang, X.F., Liu, Z.G., Shen, W. and Gurunathan, S., 2016. Silver nanoparticles: Synthesis, characterization, properties, applications, and therapeutic approaches. *Int. J. mol. Sci*., **17**: 1534. https://doi.org/10.3390/ijms17091534

Zhao, L., Qi, S. and Zheng, J., 2019. Mechanistic insights into the antifungal activity of silver nanoparticles against *Candida albicans*. *Microb. Pathog*., **128**: 150-156.